This is the accepted version of Parolari et al., C- and O-Band Operation of RSOA WDM PON Self-Seeded Transmitters up to 10 Gb/s [Invited], JOURNAL OF OPTICAL COMMUNICATIONS AND NETWORKING, 2015, 7-2: A249-A255.
The final publication is available at http://dx.doi.org/10.1364%2FJOCN.7.00A249

# C- and O-Band Operation of RSOA WDM PON Self-Seeded Transmitters up to 10 Gb/s [Invited]

Paola Parolari, Lucia Marazzi, Marco Brunero, Mario Martinelli, Romain Brenot, Anaelle Maho, Sophie Barbet, Giancarlo Gavioli, Gael Simon, Sy Dat Le, Fabienne Saliou, and Philippe Chanclou

***Abstract*—We propose a network-embedded colorless self-tuning transmitter for wavelength division multiplexed (WDM) networks based on self-seeding in reflective semiconductor optical amplifiers (RSOAs). We compare up to a 10-Gb/s data rate in either O-band or C-band operation. In particular, the transmitter exploits a two-Faraday rotator configuration to ensure polarization-insensitive operation and allowing for the exploitation of high-gain C- and O-band RSOAs, which present a very high polarization-dependent gain. Two different multiplexers and various lengths of drop fibers constituted the network-embedded transmitters in order to evaluate various dispersion load influence on cavity buildup. Moreover, transmission over standard single-mode feeder fiber has been evaluated both at 2.5 and 10 Gb/s to compare the performance in both bands, confirming the absence of chromatic dispersion penalties for the O-band operation.**

***Index Terms*—Chromatic dispersion; Colorless optical transmitter; Reflective semiconductor optical amplifier (RSOA); WDM passive optical networks (PON).**

## I. Introduction

Wavelength division multiplexed (WDM) passive optical networks (PONs) can offer a pair of wavelengths per user achieving point-to-point connectivity and allowing the fiber-transmission medium to be shared while supporting independence of multiple access protocols. Although this feature was not sufficient to let pure WDM PON become the solution for the fiber-to-the-home (FTTH) access residential market, it could be very useful to support future mobile-access applications. In particular, optical multiplexing technologies can represent an efficient solution for the fronthaul network segment, which links the remote radio-heads (RRHs), where the analogue amplification is performed at the antenna site, and the baseband units (BBUs), where the baseband digital processing is separately performed. The exploitation of digital radio over fiber (D-RoF) allows the BBUs to be centralized in a central office, data center, or base-station hotel, as in a cloud-computing model, the cloud radio access network (C RAN), which can be connected to several corresponding RRHs by means of optical fibers [1]. The fronthaul link thus transports the high-bit-rate digitized radio signal, which natively includes the synchronization signal, with standard interfaces such as the Common Public Radio Interface (CPRI). CPRI has stringent low-latency requirements, symmetrical bit rates ranging from 614.4 to 10137.6 Mb/s for upstream and downstream, and a strong requirement on jitter.

Actually, the simplest optical distribution network between RRHs and BBUs can be achieved by point-to-point fibers, but this solution is expensive in terms of the number of fibers per antenna site due to the high RRH number. To allow an efficient transport of several RRH-BBU links on a limited number of fibers a multiplexing technique is thus needed. The WDM-PON solution is in principle able to support any protocol, and it is compatible with all data rates and with the limited and controlled latency of fronthaul. Moreover, the exploitation of a colorless transceiver would overcome inventory problems, which could burden the mobile-network administration, limiting inventory and maintenance costs [2]. Furthermore, self-tuning transceivers, i.e., able to automatically and passively assign the source wavelength per the optical infrastructure, would avoid the main drawback of the wavelength assignment policy.

In this paper we propose WDM-PON transceivers based on self-seeded optical sources, which are both colorless and self-tuning. Avoiding external sources, they do not suffer from any backscattering, and the presence of an external cavity in principle should allow promising performance both in terms of power budget and of ultimate bit rate [3]. In particular, we present a comparison between network embedded self-tuning colorless transmitters, based on a self-seeding architecture exploiting high polarization-dependent gain (HPDG) reflective semiconductor optical

Manuscript received July 1, 2014; revised October 2, 2014; accepted October 16, 2014; published December 1, 2014 (Doc. ID 214950).

P. Parolari (e-mail: paola.parolari@polimi.it), L. Marazzi, M. Brunero, and M. Martinelli are with Politecnico di Milano, Dip. Elettronica Informazione e Bioingegneria, Milan 20133, Italy.

R. Brenot, A. Maho, and S. Barbet are with III-V Lab, a joint lab of Alcatel-Lucent Bell Labs France, Thales Research and Technology, and CEA Leti, Marcoussis 91460, France.

G. Gavioli is with Alcatel-Lucent Italia, Vimercate, Milano, Italy.

G. Simon, S.-D. Le, F. Saliou, and P. Chanclou are with Orange Labs, Lannion 22307, France.

amplifiers (RSOAs) in the C- and O-bands. Due to the presence of HPDG devices, a two-Faraday rotator (FR) topology is exploited to ensure stability of the signal state of polarization (SOP) within the optical cavity, which is established between the optical reflector at the remote node (RN) and the mirror at the reflective semiconductor optical amplifier, placed at the optical network unit (ONU) [4]. The network embedded self-tuning colorless C- and O-band transmitters share the remaining passive part of the cavity. The already available WDM-PON arrayed waveguide grating (AWG) cyclic transfer function extends its replica to the O-band, with losses equivalent to those in the C-band. Moreover, to allow for the optical distribution network (ODN) fiber plant reuse, which is unavoidable in already deployed infrastructures, the drop and feeder fibers are standard single-mode fibers (SSMF). This choice clearly raises an issue for high-bit-rate comparison between C- and O-band transmitters as it has been shown that, due to the chirp, dispersion loads significantly affect the 10-Gb/s performance in terms of reach, i.e., feeder-fiber length and cavity length, i.e., ONU distance from the RN, which is the drop fiber length [5,6].

Section II describes the high-performance RSOAs developed both in C- and O-bands to support the operation of the network-embedded transmitters. Section III presents the experimental setup employed to perform the comparison among the self-seeded transmitters when varying the drop- and feeder-fiber lengths, the AWG shape, and the full-width at half-maximum (FWHM). Section IV shows the experimental results at various bit rates, evidencing limits arising from chromatic dispersion (CD) impairments both on cavity buildup and on overall transmission. Finally, in Section V, concluding remarks are given.

## II. RSOA Chips for Self-Seeding Transmitters

The RSOA is the cavity active element and it sustains the cavity lasing, overcoming the overall cavity losses; it is also the modulating element, through direct modulation of the active chip current. Finally, the RSOA allows recirculating modulation cancellation through the self-gain modulation mechanism, supporting new signal modulation [7]. RSOA chips able to perform this triple role thus need to provide a very large gain, typically exceeding 20 dB even in deep saturation, to present a wide electro-optical (E/O) bandwidth and to perform efficient, high-speed gain compression.

Multiquantum well (MQW) devices proved to provide the best compromise between high-speed direct modulation, high gain, and efficient gain compression. C-band and O-band RSOA chips have been fabricated with III–V Labs Buried Ridge Stripe technology, from compressively strained InGaAsP MQW, with front-facet reflectivity below 60 dB and rear-facet reflectivity around 30% [8]. The ridge width and the spot-size converter design as well as the barrier height have been adapted to the operation-wavelength band in order to optimize the chip design. The realized chips offer a high small signal gain (above 25 dB) at 1.53 and 1.32 μm, respectively, for C- and O-band chips, while displaying a HPDG (higher than 20 dB). The RSOA spectra are centered around 1535 and 1320 nm and present gain ripples higher than 5 dB.

Recirculating modulation cancellation properties proved to be analogous for both C- and O-band devices, whereas due to nonradiative recombination processes, such as the Auger effect, which is known to decrease at larger gap energies, the carrier lifetime is much higher in the O-band RSOAs. This induces a difference between the two RSOAs in terms of modulation bandwidth. Figure 1 presents a comparison between the measured E/O responses: The bandwidths are close to 2 and 4 GHz, respectively, for O- and C-bands. Despite the limited E/O response, direct modulation up to 10 Gb/s is sustainable, as demonstrated by Fig. 2. Directly modulated amplified spontaneous emission (ASE) eye diagrams at 10 Gb/s are shown for the C-band [Fig. 2(a)] and O-band [Fig. 2(b)], evidencing, as expected, some amount of intersymbol interference.

## III. Experimental Setup

The colorless self-tuning network embedded architecture is presented in Fig. 3. The transmitter relies on a laser cavity, which is constituted by an RSOA active chip, placed at the ONU, whose reflective end is one of the cavity mirrors, the drop fiber, which connects the ONU and the RN, the RN multiplexer, an output coupler, and a mirror also placed at the RN. The optical multiplexer is the cavity wavelength-selective element: Each cavity associated with the single multiplexer channel will emit at the channel wavelength, self-tuning itself [3]. As the employed high-performance RSOAs present more than 20-dB PDG the architecture contains a FR, located in close proximity to the RSOA output, and a FR mirror (FRM), shared by all ONUs and placed at the RN close to the AWG. Thanks to the FR property it has been demonstrated [4] that at the RSOA input the state of polarization is stably retraced and aligned with the RSOA high-gain transverse mode, showing a high degree of polarization. In order to get the proper rotation (i.e., 45°) the FRs work either in the C-band or

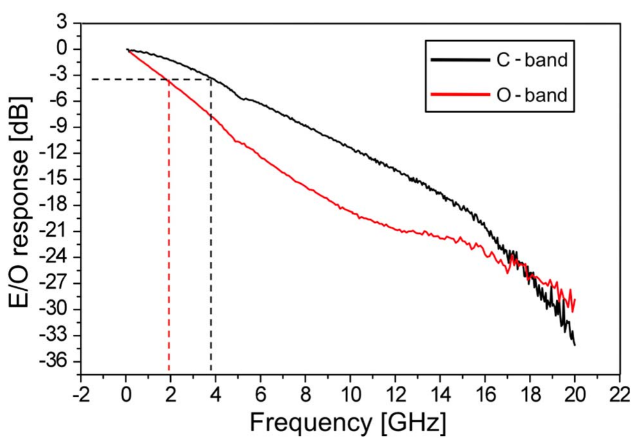


Fig. 1. Measured E/O bandwidth for C- and O-band RSOAs for 100 mA bias current and direct amplified spontaneous emission (ASE) small-signal modulation.

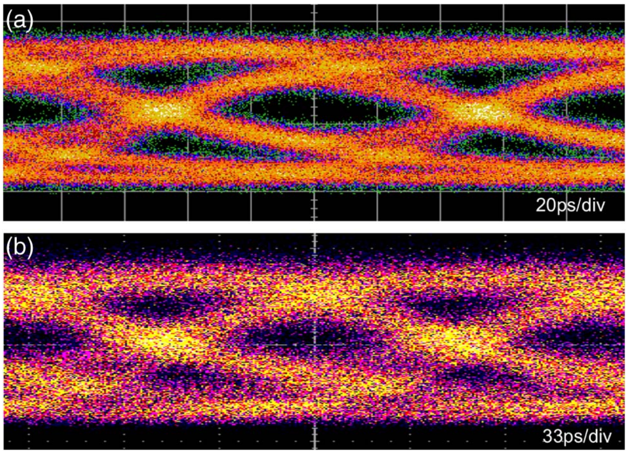


Fig. 2. Eye diagrams of directly modulated ASE at 10 Gb/s at the RSOA output: (a) C-band RSOA, (b) O-band RSOA.

O-band [9]. The feeder fiber connects the cavity output coupler with the central office (CO) receiver, which is constituted by an avalanche photodiode (APD) receiver followed by a clock and data recovery circuit (CDR). In the case of 10-Gb/s measurements the commercially available CDR also features an electronic equalizer, namely a 9-taps feed-forward equalization (FFE) and a 4-taps decision-feedback equalization (DFE). Both drop and feeder fibers are SSMF with length up to 1 km for the drop fiber and up to 70 km for the feeder fiber. Various setup elements have been used as a RN wavelength multiplexer: a 32-channel Gaussian athermal cyclic AWG designed for C-band 100-GHz channel spacing, which presents a FWHM of 55 and 65 GHz, respectively, in the C- and O-band; a programmable optical filter, which mimics the Gaussian AWG transfer function with various FWHMs in the C-band; and two flat-top AWG filters with 100 and 200 GHz FWHM, respectively, in the C- and O-bands. The filters present different FWHMs and different insertion losses: The Gaussian AWG has almost the same losses in both bands equal to 4 dB as the programmable optical filter; the C-band flat-top AWG shows an insertion loss (IL) of 1.5 dB, whereas the O-band IL is nearly 3 dB. By adding a fixed 2-dB loss in the measurements with the C-band flat-top AWG, we have been able to compare cavities with nearly equal associated roundtrip losses, although the splitting ratio for the C-band cavities was 80/20, whereas for the O-band it was 90/10. Therefore the difference in IL is around 0.5 dB due to the O-band's slightly higher fiber attenuation and to the fact that 20% and 10% of the optical power is respectively output to the feeder fiber. These losses range from 11–12 dB for very short cavities (around 10-m drop fiber) to 13–15 dB for the 1-km long drop fiber. Consequently, the analyzed transmitters present different associated relative intensity noises (RINs) [6,10] and in particular, given a certain working point defined by the bias current, due to the roundtrip losses, they provide different output powers, i.e., different available power budgets for transmission in the feeder fiber.

As an example Fig. 4 shows the power (measured at the cavity output, (Fig. 3 point A) versus bias-current curves

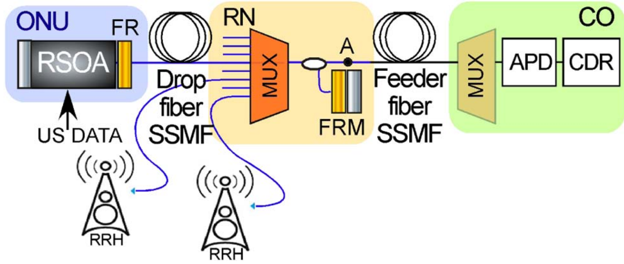


Fig. 3. Experimental setup of the colorless self-tuning transmitter: optical network unit (ONU), remote radiohead (RRH), remote node (RN), multiplexer (MUX), and central office (CO).

for the cavities exploiting the Gaussian AWG and drop fibers of 10-m and 420-m SSMF. It can be seen that the output power is almost the same for the different cavity lengths, whereas the C-band curves present a slightly higher threshold: 35 mA compared to 24 mA of the O-band, which is due to the different roundtrip losses (which differs by nearly 1.5 dB), mainly for the output coupling, and to higher ASE power and lower saturation power of O-band RSOAs. Given that the working point of the transmitters is around 110 mA the available output power for transmission in the feeder fiber is nearly –5.5 dBm and –7.5 dBm, respectively, for the O-band and C-band.

## IV. Experimental Results

We first discuss results at 2.5 Gb/s obtained both in the C- and O-band exploiting the flat-top AWGs. Figure 5 in particular displays the comparison between the performances in the two bandwidths for a 10-m SSMF cavity.

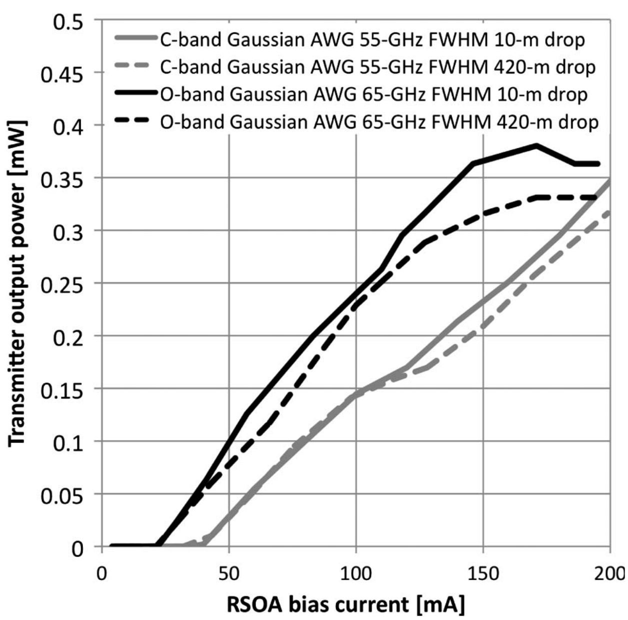


Fig. 4. Output power (point A in the set up) as a function of the RSOA bias current for the transmitter with Gaussian AWG: black lines are for O-band, gray lines for C-band, 10-m drop fiber cavities have continuous lines, whereas 420-m drop fiber cavities have dashed lines.

By comparing the square curves, it can be seen that back-to-back performance down to $10^{-5}$ bit error rate (BER) is similar, as the extinction ratios (ERs) of the C- and O-band transmitter are comparable and equal, respectively, to 5 and 6 dB. On the other hand, the C-band back-to-back curve presents an error floor at $10^{-7}$, whereas the O-band performance is error-free. The error-floor rising is mainly due to the tighter AWG spectral filtering, which results in an increased RIN [6]. Where propagation in the SSMF feeder fiber is concerned (circle and triangle curves), it is evident that no CD penalty is present for the O-band transmitter, whose bridged distance is limited only by the available output power to nearly 72 km (diamonds), whereas already at 2.5 Gb/s the C-band transmitter suffers from non-negligible CD penalties and 50-km SSMF shows an error floor of $10^{-4}$ BER due to the interplay between CD and the chirp associated with the output signal [11]. Figure 6 presents the same comparison for a 1-km SSMF cavity. Only a slight penalty can be registered with respect to the short cavity both for the C- and O-band, confirming data obtained up to 5-km SSMF cavities and presented in Ref. [12]. Again, O-band performances are just power-budget limited, whereas C-band performances are CD limited.

Figure 7 presents the comparison in the two bands for Gaussian AWG-based cavities with drop fibers of 420 m. The ER of 5.7 dB is obtained with a bias current around

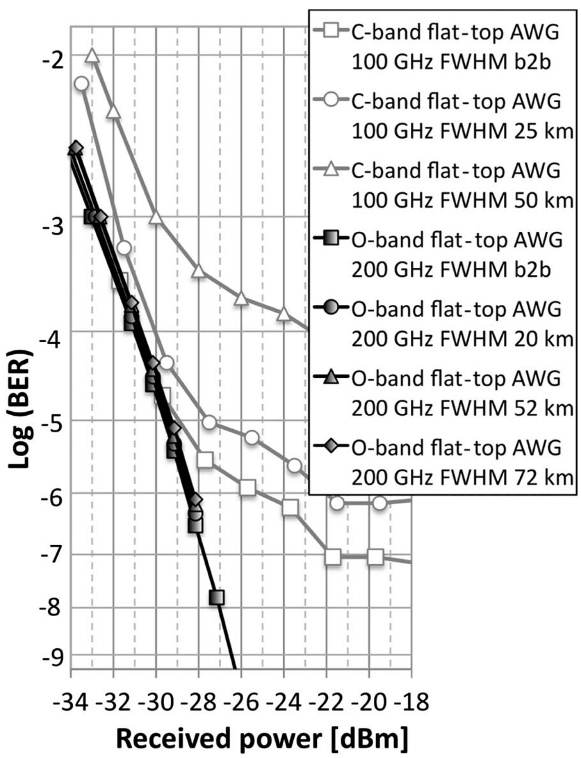


Fig. 5. BER measurements at 2.5 Gb/s for flat-top AWG-based cavities with 10-m SSMF drop fiber in back-to-back (squares), after propagation in 20-km SSMF (circles), in 50-km SSMF (triangles), and in 72-km SSMF (diamonds). Full black symbols are for O-band with 200-GHz FWHM AWG, and open gray symbols are for C-band with 100-GHz FWHM AWG.

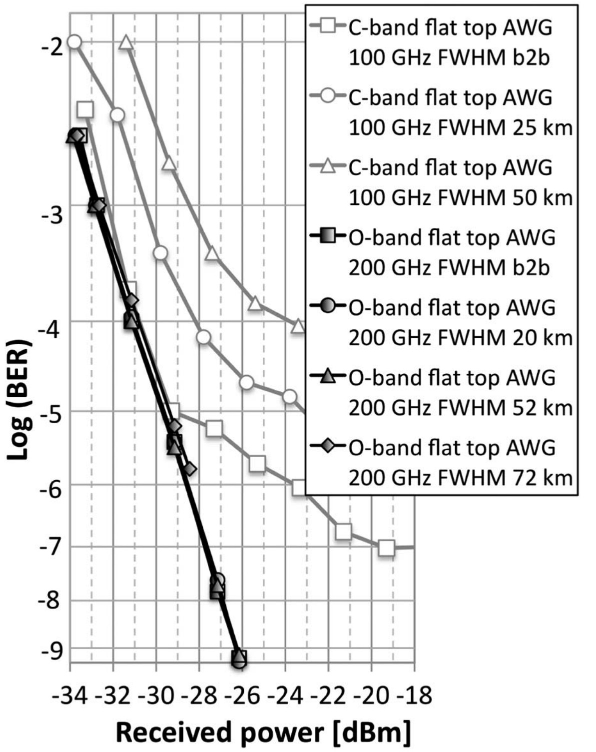


Fig. 6. BER measurements at 2.5 Gb/s for flat-top AWG-based cavities with 1-km SSMF drop fiber in back-to-back (squares), after propagation in 20-km SSMF (circles), in 50-km SSMF (triangles), and in 72-km SSMF (diamonds). Full black symbols are for O-band with 200-GHz FWHM AWG and open gray symbols are for C-band with 100-GHz FWHM AWG.

108 mA and 2.6 V peak-to-peak data voltage in both bands. As C-band operation is concerned (gray curves), negligible penalties are present, down to $10^{-4}$ BER, in back-to-back between the transmitters exploiting the 110-GHz and 55-GHz FWHM AWG. The 55-GHz FWHM AWG-based transmitter nevertheless shows an increased error floor rising from lower than $10^{-9}$ to $5 \times 10^{-7}$ due to the tighter AWG spectral filtering, which, as previously stated, results in increased RIN on the transmitter output signal and thus impacts system performance. After 10-km transmission over SSMF, performances worsen for the 110-GHz FWHM AWG, while with the tighter AWG filtering the error floor reaches a $10^{-6}$ BER. After 24-km SSMF transmission, the transmitter with both AWGs shows an error floor above a $10^{-6}$ BER. With an increased dispersion load, corresponding to 24-km SSMF propagation, the performance difference between the two AWG-based cavities is reduced, as can be seen comparing the two BER curves with open and full circles, respectively, in Fig. 7 for the 110-GHz FWHM and the 55-GHz FWHM. The transmitter exploiting wider filtering exhibits a wider modulated output optical spectrum, which is as a consequence more affected by the accumulated dispersion load. It can be thus concluded that, after 24-km SSMF, the accumulated chromatic dispersion becomes the limiting factor for the system performance in the C-band. On the other hand, the O-band transmitter (black curves) shows no propagation penalty

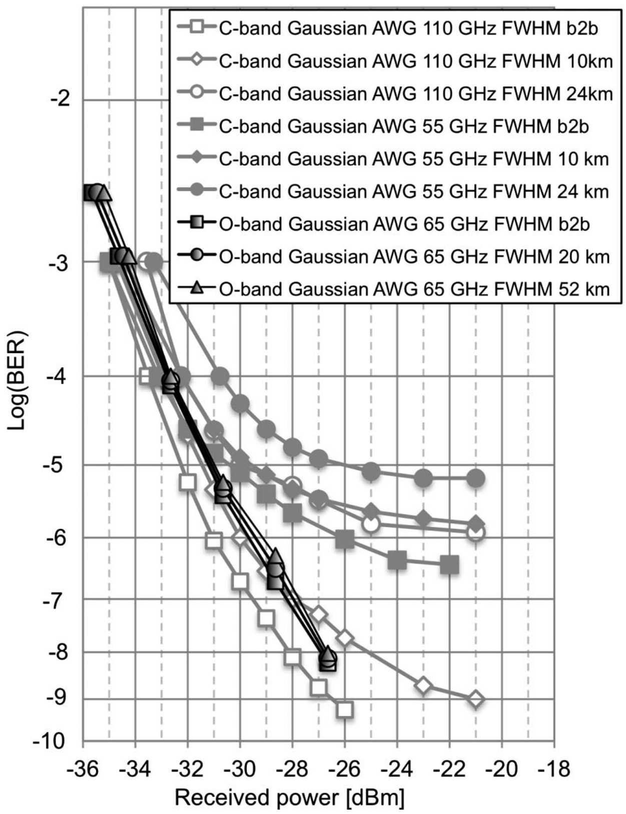


Fig. 7. BER measurements at 2.5 Gb/s for Gaussian AWG-based cavities with 420-m SSMF drop fiber in back-to-back (squares), after propagation in 10-km SSMF (diamonds), in 20-km SSMF (circles), and in 52-km SSMF (triangles). Full black symbols are for O-band with 65-GHz FWHM AWG, open gray symbols are for C-band with 110-GHz FWHM AWG, and full gray symbols are for C-band with 55-GHz FWHM AWG.

up to 52-km SSMF, achieving longer transmission reach. Back-to-back performance is not very different from those of the two C-band transmitters, down to a $10^{-4}$ BER due to similar ERs, as it has been previously evidenced for the flat-top AWG based transmitters. The previous 2.5-Gb/s measurements evidenced performance well below the forward-error correction (FEC) threshold [13], so that the required 7% increase in data rate would just add minor power penalties, not preventing successful correction to a $10^{-12}$ BER and obtaining error-free operation.

Figure 8 presents the 10-Gb/s back-to-back BER performance for the Gaussian AWG-based cavities with 420-m SSMF drop fiber; the flat-top AWG in fact has not allowed operation at 10 Gb/s with performance below a $10^{-2}$ BER. The bias currents have been optimized in both bands, leading to ERs of 5.5 and 4.3 dB, respectively, for the C-band and O-band. Due to the quite similar ERs, the two curves show analogous performance at a $10^{-3}$ BER, but despite the wider cavity filter, which should allow lower associated RIN, the C-band BER curve presents a $10^{-4}$ floor compared with the lower than $10^{-7}$ floor of the O-band transmitter. At 10 Gb/s there is stronger evidence, with respect to 2.5-Gb/s results, that the CD inside the cavity (i.e., due to the drop fiber) highly influences the BER performance, due to the presence of high mode-partition noise levels [14]. Thus, the O-band transmitter, accumulating almost null CD in SSMF, is favored with respect to the C-band one. The impact of CD influencing cavity buildup is also confirmed by the analysis of the output spectra, which are presented in Fig. 9. As the two cavities exploit AWG with different FWHMs, we choose to compare the spectra FWHMs normalized with respect to the AWG FWHMs: It can be seen that despite the normalization coefficient being lower for the O-band, the spectrum achieved in this band is less affected by the buildup in the drop fiber, confirming the previous discussion. Figure 8 also presents BER curves after propagation in 20-km feeder fibers (triangles). In order to compare distance with equal dispersion loads C-band propagation has been performed in dispersion-shifted fiber (DSF), whereas O-band propagation was in SSMF. As expected, when accumulating almost zero dispersion, both transmitters present performance close to back-to-back. On the other hand, if the ODN fiber plant is to be reused, in addition to cavity buildup advantages, the O-band transmitter outperforms the C-band transmitter in SSMF feeder fiber transmission, as already demonstrated by the 2.5-Gb/s results. In particular, at 10 Gb/s the C-band transmitter tolerates around 80 ps/nm positive dispersion load,

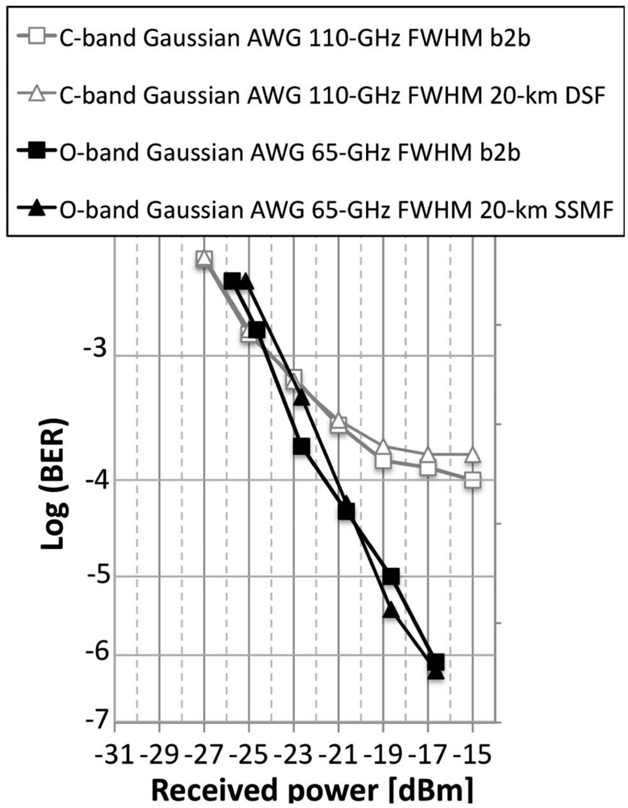


Fig. 8. Back-to-back (squares) and after 20-km transmission (triangles) BER measurements at 10 Gb/s for Gaussian AWG-based cavities with 420-m SSMF drop fiber. Black symbols are for O-band with 65-GHz FWHM AWG, and open gray symbols are for C-band transmitter with 110-GHz FWHM AWG.

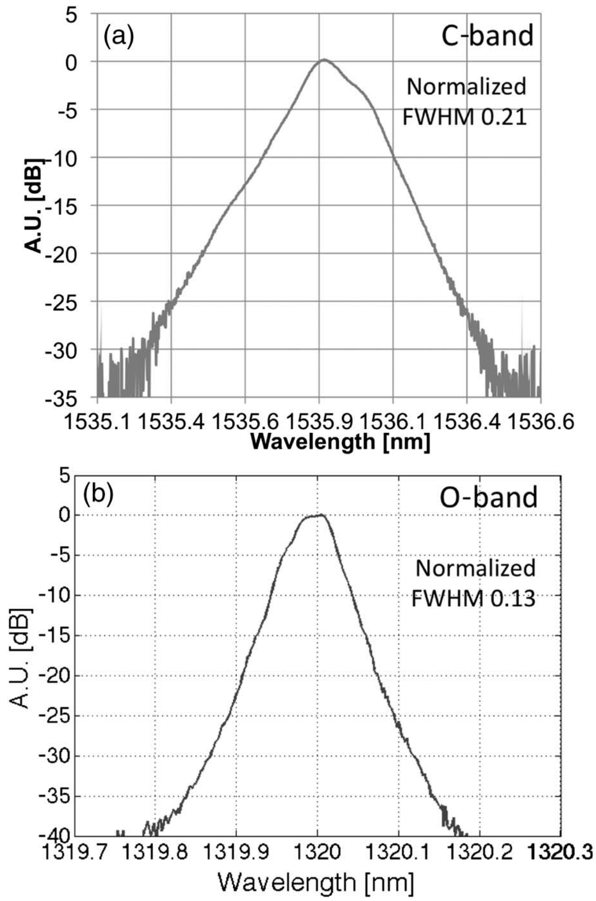


Fig. 9. Modulated spectra at 10-Gb/s eye: (a) C-band operation and (b) O-band operation. The modulated spectra are measured with an optical spectrum analyzer with 10-pm resolution.

bridging just a few kilometers of SSMF [5], whereas the O-band transmitter supports transmission over more than 40-km SSMF at a $3 \times 10^{-3}$ FEC limit [15].

## V. Conclusion

We have compared operation of up to 10 Gb/s of network-embedded colorless self-tuning WDM transmitters for fronthaul access applications, which exploit self-seeding in either C-band or O-band RSOAs. Exploitation of cyclic AWGs, as previously demonstrated for the Gaussian AWG, allows the two transmitters to leverage on the same ODN including SSMF, yet the FRs, necessary to use the HPDG RSOAs, feature a band-dependent operation. The transmitter performances have been experimentally evaluated for various drop fiber lengths, which characterize the transmitter cavity together with the WDM multiplexer, which has been supplied either by Gaussian AWGs or flat-top AWGs. Comparison of measurements in back-to-back at 2.5 and 10 Gb/s evidenced the impact of CD also on cavity buildup; due to the enhancement of the mode-partition noise, in the presence of a non-negligible dispersion load, O-band transmitters displayed better performance with error floors below a $10^{-9}$ BER. Nonetheless, at 2.5 Gb/s the C-band transmitter demonstrated support of up to 5-km drop fiber [16], whereas the O-band demonstrated up to 26-km drop fiber [17], the limiting factor being CD in the C-band and cavity losses and RIN in the O-band. At 10 Gb/s, cavity lengths were limited to 400 m by CD in the C-band and to 1 km in the O-band by both losses and RIN [15]. Moreover, after propagation over tens of kilometers of SSMF the O-band transmitters have confirmed the absence of chromatic dispersion penalties; thus their performance is only limited by the power budget, which specifically allowed transmission over more than 70-km and 40-km SSMF, respectively, at 2.5 and 10 Gb/s. On the contrary C-band operation is limited by CD accumulation, allowing bridging around 50-km SSMF at 2.5 Gb/s and less than 10 km at 10 Gb/s with a BER lower than the $3 \times 10^{-3}$ FEC limit. These results are encouraging in view of possible self-tuning transmitter exploitation in the mobile fronthaul in O-band for already deployed ODN and in C-band in green-field deployments with low dispersion fiber exploitation. Nevertheless, due to the requirement of a $10^{-12}$ BER for CPRI applications, possible BER floors should be avoided. Thus, in future works, the encapsulation of CPRI inside a framing with forward-error correction will be considered, taking into account the trade-off between latency and BER performance.

## Acknowledgments

This work was supported in part by the European Union's Seventh Framework Programme (FP7/2007-2013) under grant agreement ERMES no. 288542 2012 and by the Italian Ministry of University and Research through the ROAD-NGN project (PRIN2010-2011).

## References

[1] P. Parolari, L. Marazzi, M. Brunero, A. Gatto, M. Martinelli, P. Chanclou, Q. Deniel, F. Saliou, S. D. Le, R. Brenot, S. Barbet, F. Lelarge, S. Gebrewold, S. O'Duill, D. Hillerkuss, J. Leuthold, G. Gavioli, and P. Galli, "Self-tuning transmitter for fibre-to-the-antenna PON networks," *Opt. Switching Netw.*, vol. 14, pp. 25–31, Aug. 2014.

[2] A. Lometti, C. Colombo, S. Frigerio, and V. Sestito, "Network architectures for CPRI backhauling," in *Proc. ICTON*, Coventry, UK, 2012.

[3] E. Wong, K. Lee, and T. Anderson, "Directly modulated self-seeding reflective semiconductor optical amplifiers as colourless transmitters in WDM PON," *J. Lightwave Technol.*, vol. 25, pp. 67–74, 2007.

[4] M. Martinelli, L. Marazzi, P. Parolari, M. Brunero, and G. Gavioli, "Polarization in retracing circuits for WDM-PON," *IEEE Photon. Technol. Lett.*, vol. 24, pp. 1191–1193, 2012.

[5] L. Marazzi, P. Parolari, M. Brunero, A. Gatto, M. Martinelli, R. Brenot, S. Barbet, P. Galli, and G. Gavioli, "Up to 10.7-Gb/s high-PDG RSOA-based colorless transmitter for WDM networks," *IEEE Photon. Technol. Lett.*, vol. 25, pp. 637–640, 2013.

[6] Q. Deniel, F. Saliou, L. A. Neto, N. Genay, B. Charbonnier, D. Erasme, and P. Chanclou, "Up to 10 Gbit/s transmission in WDM-PON architecture using external cavity laser based on self-tuning ONU," in *Proc. OFC/NFOEC*, Los Angeles, CA, 2012, paper JTh2A.55.

[7] L. Marazzi, P. Parolari, R. Brenot, G. de Valicourt, and M. Martinelli, “Network-embedded self-tuning cavity for WDM-PON transmitter,” *Opt. Express*, vol. 20, pp. 3781–3786, 2012.

[8] J.-Y. Emery, T. Ducellier, M. Bachmann, P. Doussiere, F. Pommereau, R. Ngo, F. Gaborit, L. Goldstein, G. Laube, and J. Barrau, “High performance 1.55 μm polarisation-insensitive semiconductor optical amplifier based on low-tensile-strained bulk GaInAsP,” *Electron. Lett.*, vol. 33, pp. 1083–1084, 1997.

[9] M. Presi and E. Ciaramella, “Stable self-seeding of reflective-SOAs for WDM-PONs,” in *Proc. OFC/NFOEC*, Los Angeles, CA, 2011, paper OMP4.M.

[10] A. D. McCoy, P. Horak, B. C. Thomsen, M. Ibsen, and D. J. Richardson, “Noise suppression of incoherent light using a gain-saturated SOA: Implications for spectrum-sliced WDM systems,” *J. Lightwave Technol.*, vol. 23, pp. 2399–2409, 2005.

[11] A. Gatto, P. Parolari, L. Marazzi, M. Brunero, S. Barbet, A. Maho, R. Brenot, G. Gavioli, P. Galli, and M. Martinelli, “Off-set filtering for enhanced transmission in RSOA based WDM-PON,” in *Proc. ICTON*, Cartagena, Spain, June 23–27, 2013, paper We.A.3.5.

[12] P. Parolari, L. Marazzi, M. Brunero, M. Martinelli, A. Maho, S. Barbet, F. Lelarge, R. Brenot, G. Gavioli, G. Simon, F. Saliou, Q. Deniel, and P. Chanclou, “Operation of a RSOA WDM PON self-seeded transmitter over more than 50 km of SSMF up to 10 Gb/s,” in *Proc. OFC*, 2014, paper W3G.4.

[13] T. Mizuochi, “Next generation FEC for optical communication,” in *Proc. OFC/NFOEC*, San Diego, CA, 2008, paper OTuE5.

[14] S. A. Gebrewold, L. Marazzi, P. Parolari, R. Brenot, S. P. O. Dúill, R. Bonjour, D. Hillerkuss, C. Hafner, and J. Leuthold, “Reflective-SOA fiber cavity laser as directly modulated WDM-PON colorless transmitter,” *IEEE J. Sel. Top. Quantum Electron.*, vol. 20, no. 5, pp. 503–511, Sept.–Oct. 2014.

[15] P. Parolari, L. Marazzi, M. Brunero, M. Martinelli, R. Brenot, A. Maho, S. Barbet, G. Gavioli, G. Simon, F. Saliou, and P. Chanclou, “10-Gb/s operation of a colorless self-seeded transmitter over more than 70 km of SSMF,” *IEEE Photon. Technol. Lett*, vol. 26, pp. 599–602, 2014.

[16] Q. Deniel, F. Saliou, P. Chanclou, and D. Erasme, “Self-seeded RSOA based WDM-PON transmission capacities,” in *Proc. OFC/NFOEC*, Anaheim, CA, Mar. 17–21, 2013.

[17] G. Simon, F. Saliou, P. Chanclou, Q. Deniel, D. Erasme, and R. Brenot, “70 km external cavity DWDM sources based on O-band self-seeded RSOAs for transmissions at 2.5 Gbit/s,” in *Proc. OFC*, San Francisco, CA, 2014, paper W3G.5.